Applied Catalysis B: Environmental 165 (2015) 369–377

Contents lists available at ScienceDirect

Applied Catalysis B: Environmental

journal homepage: www.elsevier.com/locate/apcatb

Effect of propene, propane, and methane on conversion and oxidation state of three-way catalysts: a microwave cavity perturbation study

Gregor Beulertz[a,b], Martin Votsmeier[b,*], Ralf Moos[a,*]

[a] Bayreuth Engine Research Center, Department of Functional Materials, University of Bayreuth, 95445 Bayreuth, Germany
[b] Umicore AG & Co. KG, 63403 Hanau-Wolfgang, Germany

ARTICLE INFO

Article history:
Received 3 July 2014
Received in revised form
24 September 2014
Accepted 26 September 2014
Available online 30 October 2014

Keywords:
Hydrocarbon conversion
Oxygen storage capacity (OSC)
On-board diagnosis (OBD)
Lambda control
Three-way catalyst (TWC).

ABSTRACT

This paper presents laboratory reactor measurements of the steady-state conversion of the pollutants CO, hydrocarbons and NO over a three-way catalyst containing ceria as an oxygen-storage component. It is shown that the presence of the saturated hydrocarbons C_3H_8 or CH_4 causes a shift in the stoichiometry of optimal conversion (CO–NO crossover) to fuel-rich compositions. The shift was more pronounced at lower temperatures and can be explained by the kinetic limitation of the hydrocarbon oxidation reaction. A microwave cavity perturbation technique was used to measure *in situ* the oxidation state of the ceria. In a first step, titration experiments were performed. The oxygen-storage level was adjusted to a predefined level by equilibration with a H_2/H_2O mixture. The experiments showed that for a given temperature, the microwave-derived signal (here the resonance frequency) correlates well with the oxidation state of ceria. The microwave cavity perturbation technique was then applied simultaneously to steady-state performance tests in the presence of different hydrocarbons. It was found that if the exhaust stoichiometry is ramped from lean to fuel rich, the CO–NO crossover point in all cases coincides with a strong decrease in the oxidation state of ceria. The correlation between the oxidation state of the catalyst and the catalytic performance is found to be independent of the catalyst temperature and the nature of the hydrocarbon. The CO–NO crossover point can be precisely determined by the microwave cavity perturbation technique. The results suggest that a microwave-based measurement may, under some circumstances, allow for a more precise control of the catalyst performance than the conventional control by lambda sensors.

1. Introduction

The conversion of the three-way catalysts (TWC) strongly depends on the stoichiometry of the exhaust mixture. In a narrow range of exhaust stoichiometry, the catalyst simultaneously converts NO, CO and hydrocarbons with a high efficiency. This range of optimal conversion (here defined as the CO–NO crossover point) is also referred to as the 'lambda window' of the catalyst. In the introductory literature, it is frequently assumed that the optimal conversion of all three pollutants occurs at an exactly stoichiometric exhaust composition [1,2]. In practice, it is found that the range of optimal conversion is shifted to slightly fuel-rich exhaust compositions. One purpose of this publication is to investigate the influence of different hydrocarbons on the position of the lambda window.

Current exhaust aftertreatment systems for gasoline vehicles use lambda sensors before and after the catalyst to control the exhaust stoichiometry in such a way that the catalyst remains within its optimal range of operation [3,4]. Since, especially during transient operation, temporary deviations of the exhaust stoichiometry are unavoidable, current three-way catalysts contain ceria as an oxygen-storage compound. The ceria can be partially reduced in a reductive atmosphere and can be reoxidized in an oxidizing atmosphere. The purpose of the lambda control is to maintain the ceria in a partially reduced state so that the catalyst can buffer momentary perturbations of the exhaust composition to the rich and to the lean [5,6]. Today, the storage level of the ceria is determined indirectly with the help of two lambda-probes—one upstream and one downstream of the TWC [7,8].

Recently, novel approaches emerged to detect directly and *in situ* the state of catalysts by measuring the electrical properties of the catalyst coating itself [9]. Two possible principles were considered:

(1) a contact method, for which the coating is applied to planar electrodes and the electrical impedance between these electrodes is measured, and

* Corresponding authors.
E-mail addresses: martin.votsmeier@eu.umicore.com (M. Votsmeier), Functional.Materials@uni-bayreuth.de (R. Moos).

http://dx.doi.org/10.1016/j.apcatb.2014.09.068
0926-3373/

(2) a non-contact method, in which the coating material is penetrated by radio frequency waves.

The impedance-based method was investigated in detail not only for TWCs [10] but also for Lean NO_x traps (LNT) [11] with good results, but the main disadvantage that prohibits any kind of serial application was the difficulty of contacting the catalysts.

The microwave-based method (also called "microwave cavity perturbation method"), however, that allows for monitoring directly the oxygen loading state of TWCs without any electrical contacts has a higher potential [12,13]. The new method measures the electrical microwave properties (permittivity and conductivity) of the catalyst. In ceria-containing systems, the electrical conductivity of the catalyst strongly depends on the oxidation state of the ceria [14]. Therefore, the method allows for a direct measurement of the filling level of the oxygen buffer. There are two purposes to this study: First, steady-state conversion measurements will be performed to study the influence of different hydrocarbons on the position of the lambda window. It will be shown that the presence of saturated hydrocarbons leads to a shift in position of the optimal conversion window of to fuel-rich compositions. Second, the microwave cavity perturbation method will be used to measure the oxidation state of ceria *in operando* during the conversion measurements. By these in situ experiments, it will be shown that there is a strong correlation between the oxidation state of the ceria and the positions of the lambda window. In addition, it will be shown by titration experiments that a clear correlation exists between the ceria oxidation state and the resonance frequency obtained by the microwave cavity perturbation method.

2. The microwave cavity perturbation technique

The TWC in its steel canning can be considered as a cavity resonator for microwaves [15]. A typical general setup is shown in Fig. 1 (from [13]). The cavity resonator may be coupled to a source and a load via simple "antennas" (e.g. short stubs), which are mounted inside the catalyst canning. Thus, the electrical properties of the catalyst device (ceramic honeycomb plus coating and oxygen storage material) can be measured from the outside.

Electrically, the cavity resonator can be considered as a microwave two-port. If one excites electromagnetic waves with the complex amplitudes a_1 (by one antenna) and a_2 (by the other antenna) and records the complex amplitudes b_1 and b_2 of the backscattered waves by the same antennas, then the wave amplitudes follow Eqs. (1a) and (1b):

$$b_1 = S_{11}a_1 + S_{12}a_2 \quad (1a)$$

$$b_2 = S_{21}a_1 + S_{22}a_2 \quad (1b)$$

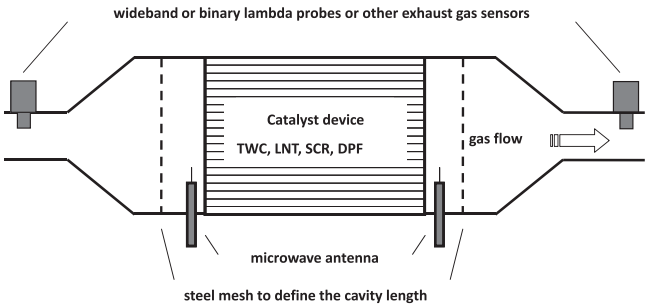

Fig. 1. Scheme of the basic setup of the microwave-based automotive catalyst state diagnosis. The steel meshes are inserted for research purposes only, to exactly define the cavity length. In serial applications they are not required. The wideband lambda probes or other exhaust gas sensors are also for research purposes only. Modified from [13].

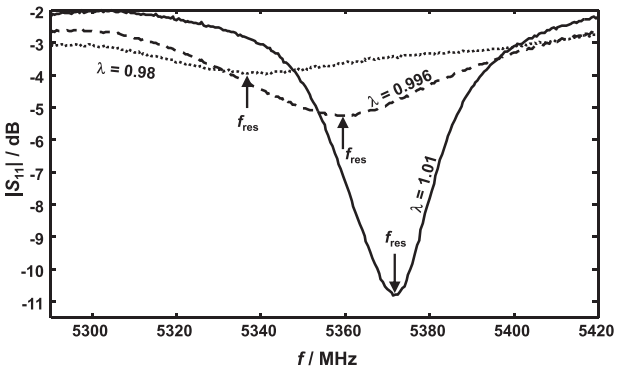

Fig. 2. Example for spectra of the absolute value of the reflection coefficients of a TWC (given in dB). Data: $T = 450\,^{\circ}C$, GHSV = 65,000 h^{-1}, TWC sample Ø 1″ × 3″ (2.54 cm × 7.62 cm), drawn curve λ = 1.01, dashed curve λ = 0.996 and dotted curve λ = 0.98. See Table 2 with C_3H_8 for detailed gas compositions. For further experimental details including setup, see [17].

In Eqs. (1a) and (1b), S_{11} is the input reflection coefficient for matched output and S_{22} denotes the output reflection coefficient for matched input. $S_{12} = S_{21}$ are the transmission coefficients, describing the energy transmission from one port to the other. In a laboratory environment, *S*-parameters are typically measured by vector network analyzers. The squared amplitude of the so-called input reflection coefficient, $S_{11} = b_1/a_1$ for $a_2 = 0$ expresses the power ratio between the reflected and the impinged wave for matched input ($a_2 = 0$). Typically, one finds a behavior as it is shown in Fig. 2 for a completely oxidized, a partially reduced, and a reduced TWC. The minima in the spectra denote resonance modes that occur at distinct resonance frequencies f_{res}. Besides the S_{11} parameters, one may also consider the transmission coefficients [12]. They yield similar results, but require two antennas.

The characteristic resonance spectrum depends on the electrical properties of the TWC (ceramic honeycomb including catalytic coating and oxygen storage material). Since the electronic conductivity of ceria–zirconia solutions depend on their degree of oxidation (from a semiconductor's point of view, the number of Ce^{3+} ions is equivalent with the number of free conduction electrons [16]), a direct catalyst state control determining the overall oxygen loading may be possible by observing the electrical properties of the catalyst.

The resonance frequency of a suitable cavity mode is a direct measure for the amount of stored oxygen. This has initially been shown by careful titrations in both engine dynamometer and laboratory test bench experiments [18,19] and will also be demonstrated below. The physical reason for the resonance frequency shifts are the increasing losses due to Ce^{3+} formation. They broaden the S_{11} curve and shift the resonance frequency [15]. The system is insensitive to other exhaust components like H_2, CO_2 or CO [20]. However, since the size of the cavity as well as the electrical conductivity of the catalyst materials depends on temperature, temperature effects on the resonance frequency have to be compensated [21]. The early studies have been conducted with Ø 4.66″ × 6″ (11.84 cm × 15.24 cm) full size catalysts, for which the first resonance modes occur at frequencies between 1.2 and 1.5 GHz. Recently, a test setup for small drilled core samples of Ø 1″ × 3″ (2.54 cm × 7.62 cm) has been described [17]. This setup, which has also been used for this work, allows high space velocities and fast temperature ramps.

3. Experimental

A test bench for Ø 1″ × 3″ TWC cores was used in this study to conduct the experiments with a pre-aged TWC (950 °C for 8 h).

Table 1
Feed gas concentrations for the light-off tests in Section 4.2, balanced with N_2.

λ	O_2 (ppm)	CO (ppm)	H_2 (ppm)	NO (ppm)	C_3H_8 (ppm)	H_2O (%)	CO_2 (%)
0.98	2498	6787	2263	1000	333	10	10
0.9969	2498	2720	907	1000	333	10	10
1.02	5678	2000	667	1000	333	10	10

Table 2
Feed gas concentrations for the stationary lambda scan tests at λ = 1 in Section 4.3, balanced with N_2.

	O_2 (ppm)	CO (ppm)	H_2 (ppm)	NO (ppm)	C_3H_6 (ppm)	C_3H_8 (ppm)	CH_4 (ppm)	H_2O (%)	CO_2 (%)
Propene	2332	2000	667	1000	333	0	0	10	10
Propane	2498	2000	667	1000	0	333	0	10	10
Methane	2833	2000	667	1000	0	0	1000	10	10

A commercial TWC with the following precious metal loading was used: 10 g/ft^3 platinum, 80 g/ft^3 palladium and 10 g/ft^3 rhodium. All tests were conducted with a constant flow rate of 2500 l/h, which corresponds to a gas-hourly space velocity of about 65,000 h^{-1}. All experiments used the same base gas mixture that contained 10% CO_2, 10% H_2O, 1000 ppm NO, and hydrocarbons (either 333 ppm C_3H_6, or 333 ppm C_3H_8, or 1000 ppm CH_4) in N_2. To adjust the normalized air–fuel ratio, λ, variable concentrations of CO, H_2, and O_2 were admixed additionally. In lean atmosphere, λ was adjusted by varying the O_2 concentration (at constant CO and H_2 concentrations), and in rich atmospheres by varying CO and H_2 concentrations (at constant O_2 concentrations). Hereby, the CO:H_2 ratio was kept constant at 3:1 and the CO concentration was always above 2000 ppm.

The full gas compositions are shown in Tables 1 and 2. From the feed gas concentrations, λ was calculated according to Eq. (2) (adapted from [22]):

$$\lambda = \frac{2X_{O_2} + 2X_{CO_2} + X_{CO} + X_{NO} + X_{NO_2} + X_{H_2O}}{2X_{CO_2} + 2X_{CO} + X_{H_2} + 9X_{C_3H_6} + 10X_{C_3H_8} + 4X_{CH_4} + X_{H_2O}} \quad (2)$$

Herein, X_i denotes the mole fraction of each component. An example to illustrate the feed gas concentration, as they depend on λ, is given in the supplementary material (Fig. S1, with additional 10% H_2O, 10% CO_2, 1000 ppm NO und 333 ppm C_3H_8). For C_3H_6 and CH_4, the O_2 feed concentration was modified accordingly (Table 2).

The conversion was calculated using the mass flow controller output data and the measured reactor outlet data (CLD (700 RE ht, ECO Physics) for NO_x; FID for total hydrocarbons, NDIR for CO and paramagnetic detector for O_2 (all installed in NGA 2000, Rosemount); hydrogen mass analyzer (MS4, H-Sense) for H_2).

The heated feed gas and the reactor temperature were adjusted to temperature, which was measured with a thermocouple upstream of the catalyst. A lambda probe (EGO sensor), operated with a voltage of 13 V, was placed downstream of the catalyst.

Microwaves were impinged by a stub-like coaxial antenna, which was located upstream of the catalyst. It was connected with a coaxial cable to the vector network analyzer (VNA Master MS2028C, Anritsu). Details can be found in [15,21].

4. Results and discussion

4.1. Titration experiments—correlation between the ceria oxidation state and the resonance frequency

In a first step, titration experiments were applied to quantitatively characterize the relationship between the storage level and the resonance frequency. The idea here is to bring the oxygen storage in a defined filling state and then to correlate the measured resonance frequency with the known oxidation state. These titration measurements are based on the fact that if the oxygen storage is in contact with an H_2/H_2O mixture, an equilibrium oxidation state is established according to the following reaction [23]:

$$Ce_2O_3 + H_2O \rightarrow 2CeO_2 + H_2 \quad (3)$$

The experiments were conducted with a constant background concentration of 10% H_2O. First, a pulse of 1.6% oxygen was used to bring the oxygen storage in a fully oxidized state. After that, a short phase with a reduced oxygen content of 700 ppm is applied for 5 s to avoid back mixing with the following H_2 pulse. During the H_2 pulse, the ceria gets reduced by H_2, leading to an H_2 consumption during the initial phase of the pulse. After some time, when an equilibrium between ceria and the H_2/H_2O mixture is established, a full breakthrough of H_2 occurred. The equilibrium oxidation state can be determined from the amount of hydrogen consumed during the initial phase of the H_2 pulse, as can be seen in the hatched area in Fig. 3.

If a microwave measurement is taken after the equilibrium has been established, the resonance frequency can be directly correlated to the oxidation state determined from the H_2-titration. The above-described pulse sequence was repeated with pulses of different H_2 concentrations between 16 and 3200 ppm. In this way, microwave-derived data at different filling levels of the oxygen storage could be taken. Fig. 4 plots the measured oxidation states versus the measured shifts in the resonance frequencies at three different temperatures. At each temperature, there exists a unique monotonous relation between the resonance frequency and the oxidation state. This means that for a known temperature, the oxidation state of the ceria can be quantitatively determined by the microwave-based method, for instance, by determining the resonance frequency.

Fig. 4 also shows that at a given oxidation state, the microwave-based signal is strongly temperature-dependent. For the fully oxidized catalyst ($x = 2$), the change in the resonance frequency amounts to about 15 MHz per 100 °C. In the steady-state experiments with different hydrocarbons discussed later in this paper, the exothermicity of the reactions caused a temperature increase

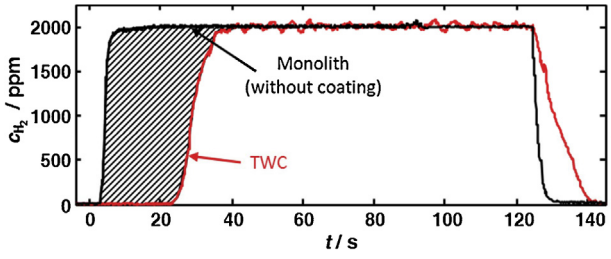

Fig. 3. Measured H_2 concentration during a typical titration experiment. Black: reference measurement using an uncoated monolith. Red: measurement with coated monolith. The amount of hydrogen required to bring the catalyst into the equilibrium oxidation state is determined from the hatched area between the two curves.

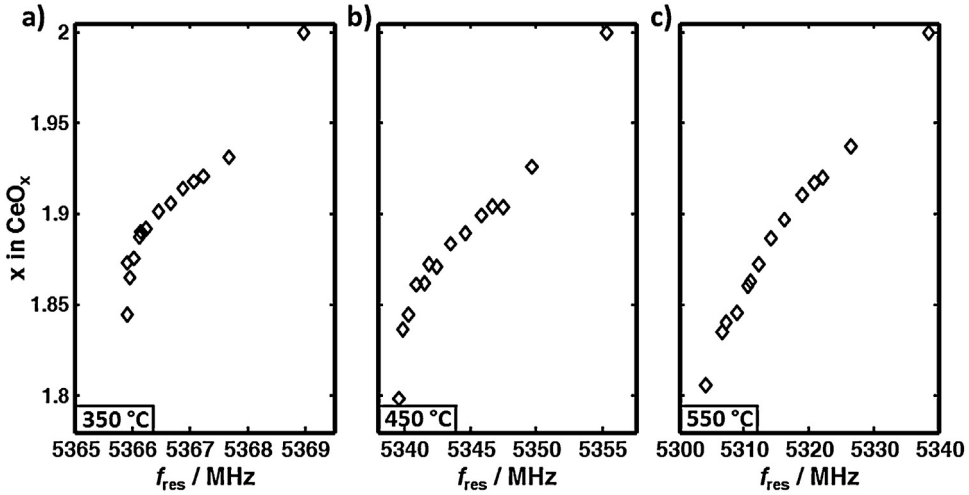

Fig. 4. The oxidation state of ceria measured by the H_2-titration versus the resonance frequency at 350 °C (a), 450 °C (b) and 550 °C (c). Each point in the plot represents the result of one pulse experiment. The point at $x = 2$ corresponds to a measurement using an O_2/H_2O atmosphere. Note the different range and scale of the abscissae of the three plots.

along the length of the catalyst of about 35 °C, corresponding to a shift in the resonance frequency of about 5 MHz, which in turn corresponds to about 30–50% of the typical change in the resonance frequency observed in the experiments.

The resonance frequency change with increasing temperature can be explained temperature-dependent increase of the electrical conductivity, as expected for an oxide semiconductor [14] in conjunction with a slight thermal expansion of the used reactor. Both effects reduce the resonance frequency. This has already been initially demonstrated in [21].

A further difficulty arises from the fact that the absolute value of the resonance frequency was found to be strongly dependent on exact position of the catalyst sample in the reactor. Since in between campaigns, the sample had to be removed from the reactor, a slightly different absolute resonance frequency was found for the same catalyst sample in different campaigns. This explains why the resonance frequencies reported later in this paper are slightly higher than the ones measured during the titration measurements. However, it was found that remounting the catalyst into the reactor only causes an offset in the measured frequencies but did never impacted the relative differences observed between different experiments.

Due to the uncertainties in the calibration of the microwave-based measurement, in the following we did not convert the measured resonance frequencies into a ceria oxidation state. Rather, we directly report the measured resonance frequencies, which are of strong interest for application in the car and which can nevertheless be seen as a semi-quantitative measure of the catalyst's oxidation state.

4.2. Light-off behavior with propane as hydrocarbon component in the feed

In order to investigate the light-off behavior, at first propane was selected as the hydrocarbon component in the feed. Three tests were carried out with a constant feed gas but different air—fuel ratios. A lean composition ($\lambda = 1.02$) and a rich one ($\lambda = 0.98$) were selected first (feed gas compositions see Table 1). An almost stoichiometric feed gas with $\lambda \approx 0.9969$ was also applied. Its air–fuel ratio corresponds to a voltage of 650 mV, as measured by the downstream lambda probe (EGO sensor) at a reactor temperature of 450 °C. C_3H_8 was selected as the hydrocarbon species. For the light-off tests, the reactor temperature was increased with a constant rate of 20 °C/min, starting at 150–550 °C. In order to have a defined state, all samples were pre-conditioned (same ramp up to 550 °C, $\lambda = 0.95$). In Fig. 5a–c, the conversion of NO, C_3H_8, CO, H_2, and O_2 is plotted as a function of temperature for three different feed gas stoichiometries. Fig. 5d shows how the resonance frequencies depend on the temperature for the three normalized air–fuel ratios. While Fig. 5a–c are typical conventional light-off curves that shall characterize the used TWC, the representation in Fig. 5d shows the effect of λ and the feed compositions on the resonance frequency, which is a measure for the degree of oxygen loading of the TWC's OSC material.

At $\lambda = 1.02$, in lean atmosphere (Fig. 5a), oxygen is available in excess at any time, which is indicated by the low O_2 conversion. The catalyst is completely oxidized and the oxygen storage component Ce is fully oxidized. The oxygen consumption at low temperature is related to H_2 oxidation (light off temperature 180 °C) followed by CO oxidation (200 °C). The NO conversion has a maximum at 195 °C. We assume that around this temperature NO is reduced by CO to form N_2O as suggested, e.g., in [24]. Above 350 °C, only about 13% NO are converted. Propane has a light-off temperature of 435 °C. The consumption of oxygen follows this curve as well.

At $\lambda = 0.98$, in rich atmosphere (Fig. 5c), oxygen is consumed and NO is reduced by H_2 and CO below 250 °C. While H_2 is nearly fully converted at 230 °C, the CO conversion curve reaches a plateau of about 79% at 250 °C as no additional oxygen is available for further oxidation. The propane oxidation starts at about 280 °C, reaches 90% conversion at 379 °C and has a light-off temperature of 340 °C. Since at temperatures above 250 °C, no oxygen can be found downstream of the TWC, the NO conversion is almost 100%. Steam reforming may be a possible explanation for the increasing C_3H_8 conversion, indicated by a higher hydrogen outlet concentration compared to the feed gas one (at 410 °C: $c_{H_2,outlet} = 4450$ ppm; $c_{H_2,feed} = 2260$ ppm).

At $\lambda = 0.9969$ (Fig. 5b), a more complex behavior occurs. Nominally, $\lambda = 0.9969$ is a slightly rich composition. At temperatures below 240 °C, H_2 ($T_{50,H_2} = 191$ °C) and CO ($T_{50,CO} = 212$ °C) are completely oxidized and the available oxygen reaches a plateau of about 40% of the feed gas value (conversion of 60%). The local maximum of the NO conversion at the CO light-off temperature indicates that CO reduces NO at temperatures between 180 and 220 °C. With increasing temperature, the oxidation of C_3H_8 increases to a propane light-off temperature of about 450 °C. At about 460 °C, a change in the trends of the curves can be seen. Above this temperature,

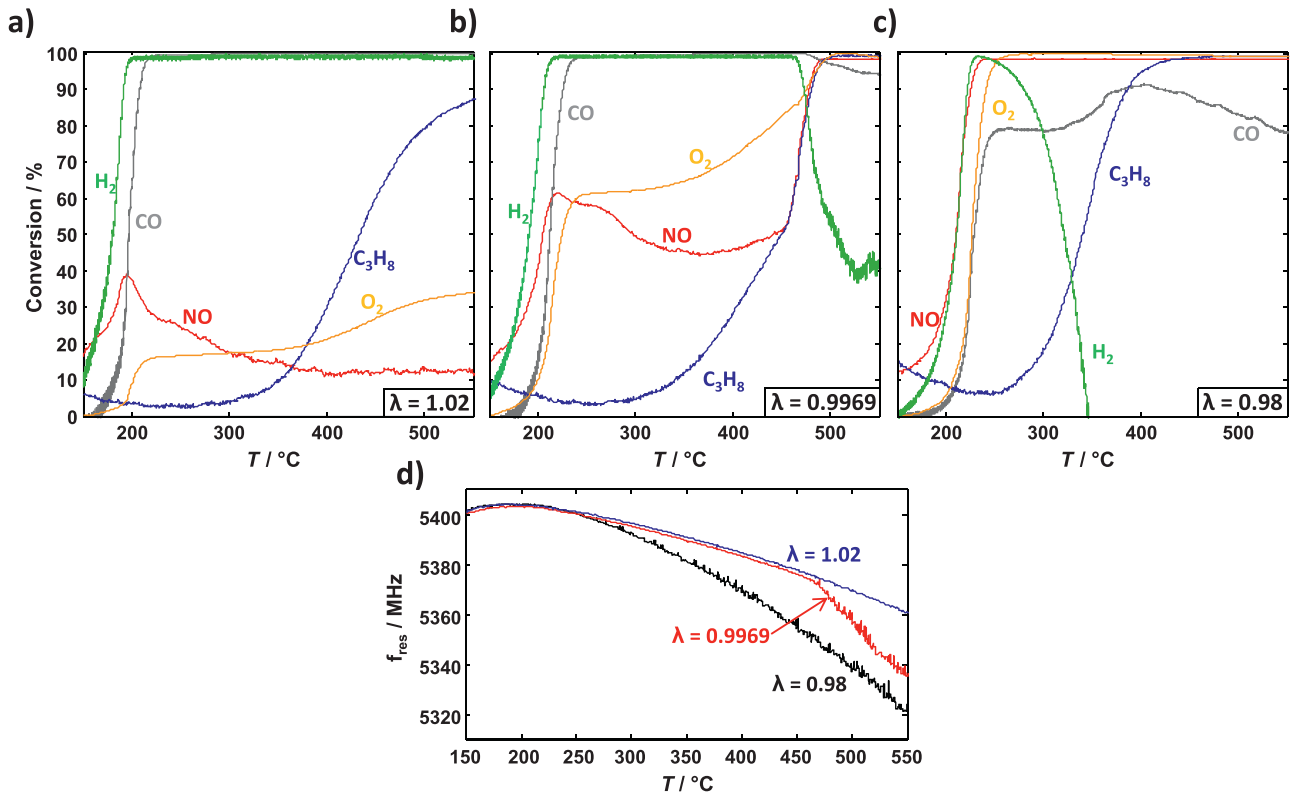

Fig. 5. Conversion of CO (grey), NO (red), H_2 (green), C_3H_8 (blue), and O_2 (orange) during light-off tests with a constant λ of the feed gas: (a) λ = 1.02, (b) λ = 0.9969, and (c) λ = 0.98; (d) corresponding resonance frequencies, f_{res}, for all three measurements.

the NO conversion and the steepness of the C_3H_8 conversion curve increase, whereas the H_2 conversion decreases, as well as the O_2 conversion increases further. Above 510 °C, almost no O_2 can be found in the outlet anymore. Below 510 °C, O_2 is available, so that the oxygen buffer is completely filled. Above 510 °C, O_2 is fully converted, so that in the absence of O_2, the ceria storage gets partially reduced. As the temperature increases further, the rate of O_2 consumption by C_3H_8 oxidation increases, leading to a further reduction of the oxygen storage. In other words, at low temperatures, C_3H_8 can be considered an inactive or 'inert' gas that does not contribute to the reaction. At higher temperatures, C_3H_8 behaves as a reductant that gets oxidized and shifts the stoichiometry from lean to rich.

The results in Fig. 5d fully support this. At low temperature, Ce is fully oxidized, independent of the gas composition. Therefore, all curves are congruent. Below 220 °C, water adsorbed on the washcoat has to be considered. Due to its higher permittivity and electrical losses, the resonance frequency decreases. Since water desorbs with increasing temperature, f_{res} increases. This explains the behavior below approx. 220 °C. Under lean conditions, the oxygen-storage component is permanently in its oxidized state. This means that only few conduction electrons are available. This yields low losses and a higher resonance frequency compared to the rich conditions. Above approximately 250 °C, the resonance frequency plots for the lean and rich feed gas split up. This temperature agrees with the starting point of oxygen consumption in Fig. 5b. Hence, above 250 °C, the kinetic limitations of the reactions cease to exist and due to the now net-reducing atmosphere, ceria is partially reduced to Ce_2O_3.

At λ = 0.9969, a different effect is observable. At temperatures below 470 °C, the resonance frequency curve behaves as it were taken in lean gas. Above this temperature, the resonance frequency decreases compared to the lean curve, since ceria is partially reduced to Ce^{3+}. This agrees with the finding of Fig. 5b that all species not being converted or only partly converted at low temperatures should be seen as inactive with respect to the TWC loading behavior. Therefore, they do not affect its oxidation state and a nominally rich atmosphere shows an oxidizing behavior. Hence, the kink in the f_{res} curve indicates the hydrocarbon light off.

4.3. *Effect of different hydrocarbons to the oxygen-storage material*

The effect that reducing species behave like an 'inert' gas, which do not affect the oxygen storage degree of the TWC, will be investigated in this section by the microwave-based method at different temperatures in different normalized air–fuel ratios from λ = 0.98 to 1.01. Initially, propane (C_3H_8) was used as a hydrocarbon species (results in Fig. 6). Later on, the more reactive propene (C_3H_6) and the more stable methane (CH_4) served as the hydrocarbon compound (Figs. 7 and 8).

Air–fuel ratio sweeps with propane, propene or methane were performed at constant feed gas temperatures of 350, 450, and 550 °C. λ of the feed gas was increased in 31 equidistant steps from 0.98 to 1.01. The amount of hydrocarbons was chosen so that in all cases the same carbon concentration was used: 333 ppm C_3H_6, 333 ppm C_3H_8 or 1000 ppm CH_4. The full gas composition for λ = 1 is given in Table 2. To obtain a lean composition, the oxygen concentration in the feed was increased for λ > 1 according to Eq. (2). To reconstruct rich exhausts, CO and H_2 were increased under a constant O_2 concentration in the feed (value of λ = 1). Their ratio remained always constant (3:1). After each step of the sweep, it was waited until the reactor reached steady-state conditions before the gas concentrations were measured downstream of the catalyst. The conversion was calculated using the MFC-output data

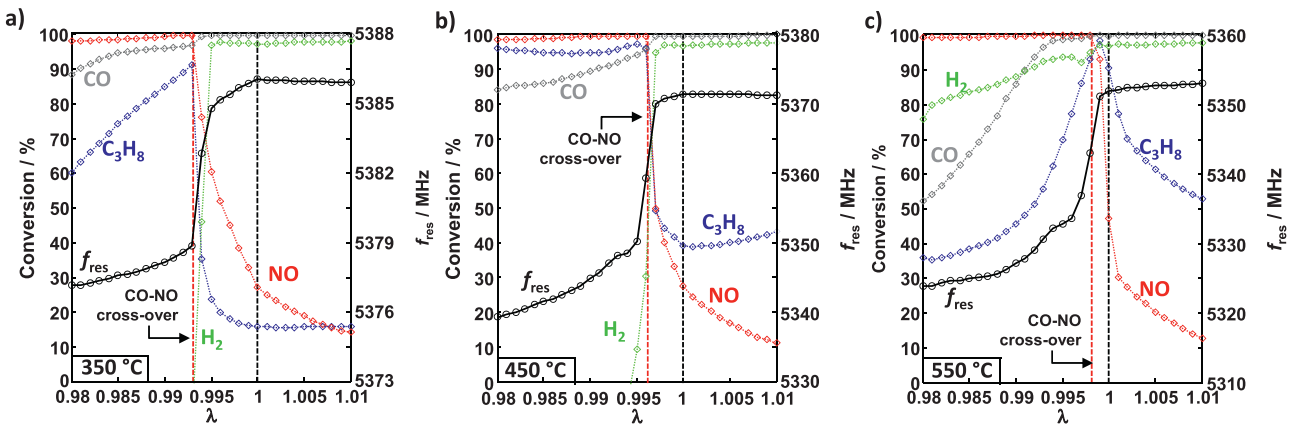

Fig. 6. λ sweep test with propane as the hydrocarbon species: steady-state conversion of NO (red), CO (grey), H_2 (green) and C_3H_8 (blue) and the corresponding resonance frequency f_{res} (black) at (a) 350 °C, (b) 450 °C, and (c) 550 °C as a function of λ. The red dashed line indicates the λ value for the NO–CO cross-over, also indicated by an arrow.

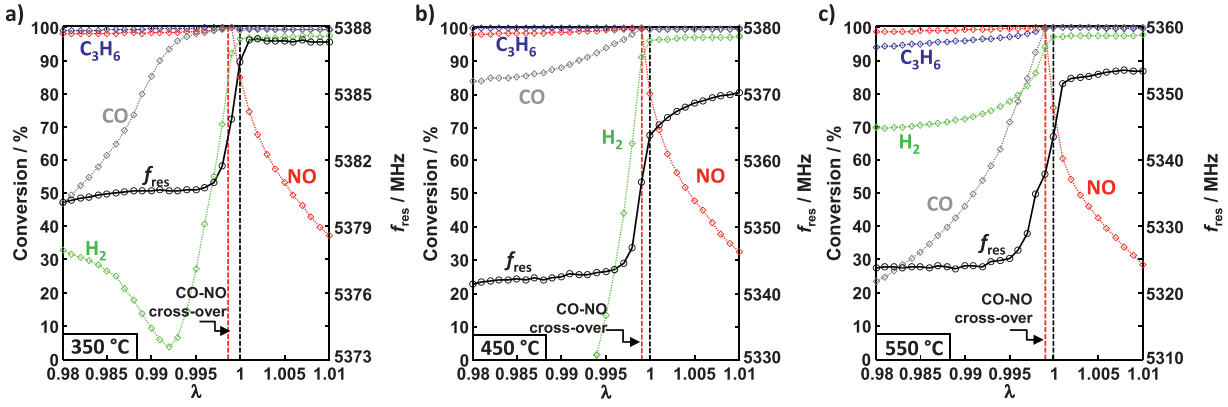

Fig. 7. Steady-state conversion of NO (red), CO (grey), H_2 (green) and C_3H_6 (blue) and the corresponding resonance frequency f_{res} (black) with C_3H_6 as the hydrocarbon component at (a) 350 °C, (b) 450 °C, and (c) 550 °C. The red dashed line indicates the λ value of the CO–NO crossover, also indicated by an arrow.

upstream and the measured concentrations downstream of the TWC as described above.

4.3.1. Results for propane

In Fig. 6, the conversion of CO, NO, and C_3H_8 as well as the resonance frequencies at 350, 450, and 550 °C are shown in dependence of the normalized air–fuel ratio λ. The measured concentrations are shown in the supplementary material in Fig. S2.

Fig. 6a shows the results obtained at 350 °C. NO is converted under rich conditions by almost 100% and decreases strongly from a distinct λ value, which can be considered as a "point of optimal conversion". The CO conversion is also almost 100% in an oxidizing atmosphere and decreases slightly in a rich atmosphere. C_3H_8 behaves differently. The conversion increases in the rich gas up to the distinct point of optimal conversion, but drops in oxidizing atmosphere below a conversion of 20%. This agrees with Fig. 5a: the light-off temperature of C_3H_8 is higher in a lean atmosphere than in a rich atmosphere.

It again becomes obvious that λ > 1 does not necessarily correspond to oxidizing conditions. Under oxidizing conditions, OSC materials are oxidized, indicated by a drop in the NO conversion directly above the point of an optimal conversion for hydrocarbons,

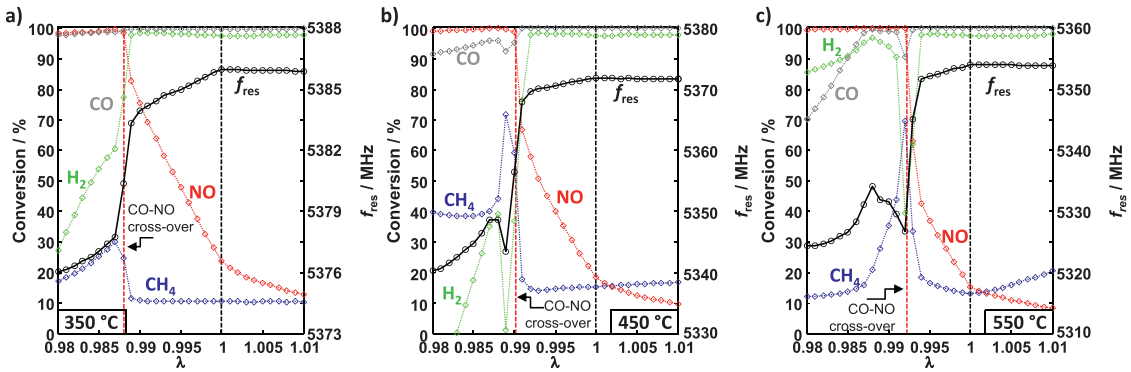

Fig. 8. Steady-state conversion of NO (red), CO (grey), H_2 (green) and CH_4 (blue) and the corresponding resonance frequency f_{res} (black) with CH_4 as the hydrocarbon component at (a) 350 °C, (b) 450 °C, and (c) 550 °C. The red dashed line indicates the CO–NO crossover, also indicated by an arrow.

CO, and NO. At 350 °C, the CO–NO cross-over (vertical red dashed line) occurs at λ = 0.993, which is significantly below the stoichiometric point at λ = 1 (vertical black dashed line). The oxidation of C_3H_8 at this temperature is kinetically limited. Hence, despite the slightly rich feed gas composition, NO cannot be reduced since the non-converted part of C_3H_8 has to be considered an 'inert' component that does not take part in the reaction. This means that the oxygen buffer should be filled.

Again, the resonance frequency reflects this behavior. It is noteworthy to mention that the resonance frequency appears to be a direct measure for the conversion. Almost exactly at the point of the CO–NO crossover, f_{res} increases sharply, i.e., as soon as the TWC is oxidized (indicated by the sharp resonance frequency increase), the conversion efficiency of C_3H_8 and NO decreases. Since the resonance frequency is a direct measure for the oxidation state of ceria, one can deduce that the conversion efficiency of a TWC is directly related to the degree of oxidation of ceria.

This behavior can also be seen at higher temperatures (Fig. 6b–c). Increasing temperature yields an increased C_3H_8 conversion under oxidizing conditions. This results in a shift of the CO–NO crossover from about λ = 0.993 at 350 °C over λ = 0.996 at 450 °C to a λ value around 0.9985 at 550 °C.

In rich feed gas, the CO conversion decreases with increasing temperature and the conversion of C_3H_8 reaches a maximum at about 450 °C. This can be explained if one has a look at the H_2 outlet concentrations. At 350 and 450 °C, H_2 is formed according to the water-gas shift reaction, which is indicated by a higher H_2 outlet concentration compared to the feed gas value, whereas H_2 is oxidized at 550 °C, resulting in a lower CO and C_3H_8 conversion.

4.3.2. Results for propene and methane

Since C_3H_8 affects largely the λ point of optimal conversion as a function of temperature and since this effect has not been seen in previous experiments without hydrocarbons and NO [17], additional experiments with the more reactive C_3H_6 (Fig. 7a–c) and the less reactive CH_4 (Fig. 8a–c) were conducted under otherwise identical conditions. The measured concentrations are shown in the supplementary material in Figs. S3 and S4, respectively.

In strong contrast to C_3H_8, C_3H_6 is fully converted at all investigated temperatures and conditions with exception of 550 °C under reducing conditions. Similar to the data with C_3H_8, under rich feed gas the CO conversion at 450 °C is higher than the one at 350 and 550 °C, which is different to the picture for H_2 conversion. H_2 shows a low conversion at 350 °C and shows a constant conversion of about 80% at 550 °C, but at 450 °C, H_2 is formed under reducing conditions. Since C_3H_6 is almost fully converted at all temperatures, there is only a negligibly small shift in the CO–NO crossover to λ = 0.999 at all temperatures. Such small shifts may also be due to inaccuracies of the used mass flow controllers. As in the case of the C_3H_8-containing feed gas, the oxidation state of ceria (as indicated by the resonance frequency) is the determining factor for the point of optimal conversion.

As expected, the more stable CH_4 has a higher light-off temperature. Furthermore, the oxidation of CO and H_2 are preferred reactions under reducing conditions. The methane conversion at λ = 0.98 and 350 °C is only 16%. It increases to 40% at 450 °C and decreases again at higher temperatures. This trend has also been observed with C_3H_8 as the hydrocarbon species and can be explained by the better H_2 conversion rate. Under net oxidizing conditions, CH_4 can hardly be converted. Even at 550 °C, only a conversion of 25% is reached.

In a narrow range around the point of optimal conversion, the CH_4 conversion increases significantly. This is less pronounced at 350 °C but becomes prominent at 450 and 550 °C. At 450 °C, in the narrow λ window of increased CH_4 conversion, a slight decrease in the CO conversion and a significant decrease in the H_2 conversion is observed. At 550 °C, this drop in the CO and H_2 conversion is even more pronounced. In contrast to the experiments with C_3H_6 and C_3H_8, the increase in CH_4 conversion goes along with a change in the oxidation state of the catalyst, indicated by a steep changing resonance frequency. With respect to the ceria oxidation, not converted CH_4 behaves like an 'inert' gas if the conditions for the CH_4 oxidation are unfavorable. These results illustrate the difficulty to control exhaust gas aftertreatment of natural gas-fuelled stoichiometrically operated vehicles. Only in a narrow stoichiometry window, which additionally shifts with temperature, methane as well as CO and NO can be removed at the same time. Using lambda probes to determine the point of optimal conversion is therefore difficult.

The difficulty in CH_4 oxidation has already been previously reported. Amongst others, Oh et al. [25] observed that over alumina-supported noble metal catalysts without ceria the conversion of CH_4 under oxidizing conditions is inhibited by higher absorption strength of O_2 at the noble metal. Below stoichiometric conditions, the CH_4 conversion rates increase due to better access of CH_4 to the reaction sites. With a decreasing amount of available oxygen in the feed gas, the oxidation is kinetically and/or stoichiometrically limited. They also report that the CH_4 conversion is reduced by adding ceria and its interaction with the noble metal sites. This can explain the results in Fig. 8a–c and might be an explanation for the low conversion of C_3H_8 (Fig. 6) and the higher light-off temperature of C_3H_8 under lean conditions (Fig. 5). It should be noted that the increase in the light-off temperature in the order C_3H_6, C_3H_8, CH_4 has already been described by other authors, for differently noble metal-loaded samples [25] as well as under consideration of the sample history [26]. Light-off temperatures increase after previous oxidation. This effect becomes markedly prominent if Pd is the main noble metal component for the CH_4 oxidation. Due to our pre-conditioning step under reducing atmospheres, we assume to have reduced effects of the sample history.

4.4. Consequences for conventional control strategies

In conventional control strategies for gasoline-fueled vehicles, two lambda probes are used: a wideband lambda probe (UEGO sensor) upstream and a binary lambda probe (EGO sensor) downstream of the catalyst. The latter is applied for trim-control and to detect malfunctions of the entire exhaust gas aftertreatment system as well as to monitor the upstream lambda probe.

The voltage of the downstream located lambda probe (EGO sensor) and the resonance frequencies of the tests with the three different hydrocarbons, C_3H_6, C_3H_8, and CH_4 (Figs. 6–8) as well as the λ points with the optimal conversion (NO–CO crossover; indicated as arrows) are plotted in Fig. 9. For clarity, only results at 450 °C are shown. The observed effects become even more marked at 350 °C and occur in a less-pronounced way also at 550 °C.

The steep drop in voltage of the binary lambda probe indicates the change from reducing to oxidizing conditions [7]. For the measurement with C_3H_6, this drop occurs at almost λ = 1. By changing the hydrocarbon component to C_3H_8 this drop shifts towards rich (λ = 0.998) and for CH_4 to lean (about λ = 1.002) conditions. These small shifts are well known and reflect cross-sensitivities of the lambda probe due to different diffusion coefficients of the gases through the porous electrodes [27]. They lead to a shift in the lambda probe characteristic. However, as can be seen from Fig. 9, in any cases the switch between lean and rich always occurs at $\lambda = (1 \pm 0.002)$.

In contrast to that, the conversion measurements with the less reactive feed components C_3H_8 and CH_4 (Figs. 6 and 8) have shown that the catalysts oxidation state and the λ points of optimal conversion may differ widely from λ = 1. It is noticeable that the points of optimal conversion, i.e. the NO–CO crossover, and the switch of

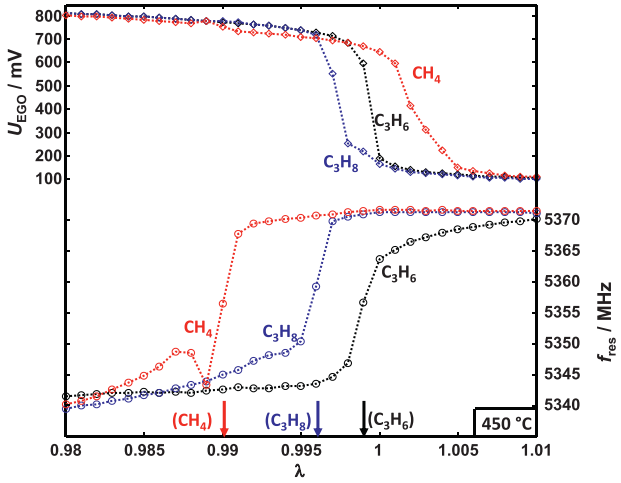

Fig. 9. Sensor signals of the lambda probe (EGO sensor) downstream of the catalyst, resonance frequencies, and the λ points with optimal conversion (NO–CO crossover; calculated from Figs. 6–8; indicated by arrows) for the tests with different hydrocarbons in the feed gas (C_3H_6 in black, C_3H_8 in blue, and CH_4 in red) at 450 °C.

the resonance frequencies—the latter indicating a changing oxidation state of ceria from the reduced (3+) state to the oxidized (4+) state—coincide. Hence, instead of measuring the gas atmosphere using lambda probes (as it is state of the art), the oxidation state of the catalyst itself should be monitored for engine control. An appropriate measure is the simple microwave cavity perturbation method. Its output signals are a function of the oxidation state of the catalyst and are well correlated with the catalyst performance. As shown in Figs. 6a–8a, this behavior is more pronounced at 350 °C, but appears at all temperatures if the hydrocarbons are not fully oxidized. Hence, the less reactive the admixed hydrocarbon species is, the more erroneous is engine control by lambda probes.

Therefore, the microwave-based method shows a remarkable potential to improve the accuracy of exhaust gas aftertreatment systems of gasoline-fueled internal combustion engines. However, despite these promising initial results, more research is required before such a system can really be applied to replace lambda probes. Influencing effects, for instance, the influence of temperature need to be further studied. At this state, it remains also unclear, how such a system behaves when the catalyst ages and loses oxygen-storage capacity which goes along with reduced conversion and increased light-off temperatures.

Whether the microwave-based direct catalyst status diagnosis will ever become ripe for mass application does not depend only on technical issues as discussed above but also on overall cost considerations.

Nevertheless, we also see a chance that the microwave-based oxygen storage detection has a potential as a diagnostic and development tool, especially for matching engine controls and emission calibration to a particular catalyst system for optimum efficiency. For that purpose, future work will focus in two directions: Using combinations of several modes and appropriate antenna configurations may lead to a spatial insight into the position of the reaction front. Further future research is directed to a more defined system, in which material properties of catalyst powders can be measured quantitatively under reaction conditions. An initial setup for that has been published recently [28].

5. Conclusion

The tests with different hydrocarbons have shown that the light-off performance of different species has an influence on the oxygen storage behavior of three-way catalysts. Species with a low conversion can be considered as 'inert' (inactive) gases, which do not reduce the oxygen storage material ceria. Therefore, especially in a low-temperature region, the ceria can be oxidized under nominally rich conditions. The λ window of optimal conversion, i.e. the NO–CO crossover, moves from $\lambda \approx 1$ for reactive propene to the rich direction. This shift gets more pronounced with decreasing reactivity of the hydrocarbon component.

The microwave cavity perturbation method was used to determine the oxygen storage directly by integrally measuring the change of the catalyst's electrical material parameters. In a first step, titration experiments were performed, where ceria was prepared in different defined oxidation states by equilibration with H_2/H_2O mixtures. The titration experiments showed that the microwave-derived signal well correlates with the oxidation state, so that the method can be used to follow the oxygen-storage level during kinetic experiments.

When the microwave-based method was applied during the steady-state conversion experiments with feeds containing different hydrocarbons, the resonance frequency correlated very well with the emissions, especially of the limited components NO, CO, and hydrocarbons. The shift of the optimal conversion window on the lambda scale is fully reflected by the resonance frequency measurements. Therefore, steady-state emissions correlate directly with the oxidation state of ceria as it has already been suggested in [22]. Cross-sensitivities to other components in the exhaust, which are a noise factor for conventional lambda sensors, are not observed with the microwave cavity perturbation method, if one considers temperatures above 230 °C, at which water is fully desorbed.

We suggest further research and development efforts to apply the microwave-based method to improve the accuracy of exhaust gas aftertreatment systems of gasoline-fuelled internal combustion engines.

Acknowledgement

This project was funded in the framework of the DFG projects MO 1060/13-1 and FI 956/5-1. R.M. gratefully acknowledges DFG grant MO 1060/13-1. The authors also would like to thank J. Schell of Umicore AG & Co. KG for assistance while conducting the experiments.

Appendix A. Supplementary data

Supplementary data associated with this article can be found, in the online version, at http://dx.doi.org/10.1016/j.apcatb.2014.09.068.

References

[1] M. Shelef, R.W. McCabe, Catalysis Today 62 (2000) 35–50.
[2] O. Deutschmann, J.D. Grunwaldt, Chemie Ingenieur Technik 85 (2013) 595–617.
[3] M. Tomforde, W. Drewelow, M. Schulalbers, Proceedings of the 16th International Conference on MMAR 24 (2011) 2–247, http://dx.doi.org/10.1109/MMAR.2011.6031352.
[4] J. Kašpar, P. Fornasiero, N. Hickey, Catalysis Today 77 (2003) 419–449.
[5] P. Kiewitz, C. Onder, L. Guzzella, Journal of Process Control 22 (2012) 984–994.
[6] C.A. Roduner, C.H. Onder, H.P. Geering, Proceedings of the 5th Mediterranean Conference on Control and Systems (1997) 1–7.
[7] J. Riegel, H. Neumann, H.-M. Wiedenmann, Solid State Ionics 152-153 (2002) 783–800.
[8] M.V. Twigg, Applied Catalysis B: Environmental 70 (2007) 2–15.
[9] R. Moos, M. Wedemann, M. Spörl, S. Reiß, G. Fischerauer, Topics in Catalysis 52 (2009) 2035–2040.
[10] S. Reiß, M. Wedemann, R. Moos, M. Rösch, Topics in Catalysis 52 (2009) 1898–1902.
[11] R. Moos, C. Zimmermann, T. Birkhofer, A. Knezevic, C. Plog, M.R. Busch, T. Ried, Sensor for directly determining the state of a NOx storage catalyst, SAE Paper 2008-01-0447, doi: 10.4271/2008-01-0447.

[12] R. Moos, M. Spörl, G. Hagen, A. Gollwitzer, M. Wedemann, G. Fischerauer, TWC: lambda control and OBD without lambda probe–an initial approach, SAE Paper 2008-01-09196, doi: 10.4271/2008-01-0916.
[13] R. Moos, G. Fischerauer, Oil and Gas Science and Technology, 2014. doi: 10.2516/ogst/2013203.
[14] H.L. Tuller, A.S. Nowick, Journal of the Electrochemical Society 126 (1979) 209–217.
[15] G. Fischerauer, M. Spörl, A. Gollwitzer, M. Wedemann, R. Moos, Frequenz 62 (2008) 180–184.
[16] M. Boaro, A. Trovarelli, J.-H. Hwang, T.O. Mason, Solid State Ionics 147 (2002) 85–95.
[17] G. Beulertz, M. Fritsch, G. Fischerauer, F. Herbst, J. Gieshoff, M. Votsmeier, G. Hagen, R. Moos, Topics in Catalysis 56 (2013) 405–409.
[18] S. Reiß, M. Spörl, G. Hagen, G. Fischerauer, R. Moos, IEEE Sensors Journal 11 (2011) 434–438.
[19] R. Moos, G. Beulertz, S. Reiß, G. Hagen, G. Fischerauer, M. Votsmeier, J. Gieshoff, Topics in Catalysis 56 (2013) 358–364.
[20] S. Reiß, M. Wedemann, M. Spörl, G. Fischerauer, R. Moos, Sensor Letters 9 (2011) 316–320.
[21] S. Reiß, Bayreuther Beiträge zur Sensorik und Messtechnik, Vol. 9, Thesis, Universität Bayreuth, Shaker-Verlag, Aachen, 2012.
[22] R. Möller, M. Votsmeier, C. Onder, L. Guzzella, J. Gieshoff, Applied Catalysis B: Environmental 21 (2009) 30–38.
[23] R.J. Gorte, S. Zhao, Catalysis Today 104 (2005) 18–24.
[24] I. Mejía-Centeno, G.A. Fuentes, Chemical Engineering Communications 196 (2009) 1140–1151.
[25] H. Se, P.J. Oh, R.M. Mitchell, Siewert, Journal of Catalysis 132 (1991) 287–301.
[26] J.R. Theis, R.W. McCabe, Catalysis Today 184 (2012) 262–270.
[27] K. Saji, H. Kondo, T. Takeuchi, I. Igarashi, Journal of the Electrochemical Society 135 (1988) 1686–1691.
[28] M. Dietrich, D. Rauch, A. Porch, R. Moos, Sensors 14 (2014) 16856–16868.